Structure and orientation of the moving vortex lattice in clean type-II superconductors

Dingping Li,[1,3] Andrey M. Malkin,[2,3] and Baruch Rosenstein[3,4]
[1]*Department of Physics, Peking University, Beijing 100871, China*
[2]*Institute of Applied Physics, Russian Academy of Science, Nizhnii Novgorod 603600, Russia*
[3]*National Center for Theoretical Sciences and Electrophysics Department, National Chiao Tung University, Hsinchu 30050, Taiwan, Republic of China*
[4]*Department of Condensed Matter Physics, Weizmann Institute of Science, Rehovot 76100, Israel*
(Received 13 February 2004; revised manuscript received 30 July 2004; published 30 December 2004)

The dynamics of the moving vortex lattice is considered in the framework of the time-dependent Ginzburg-Landau equation neglecting the effects of pinning. At high flux velocities the pinning dominated dynamics is expected to crossover into the interactions dominated dynamics for very clean materials recently studied experimentally. The stationary lattice structure and orientation depend on the flux flow velocity. For relatively velocities $V<V_c=\sqrt{8\pi B/\Phi_0}/\gamma$, where γ is the inverse diffusion constant in the time-dependent Ginzburg-Landau equation, and the vortex lattice has a different orientation than for $V>V_c$. The two orientations can be desribed as motion "in channels" and motion of "lines of vortices perpendicular to the direction of motion." Although we start from the lowest Landau level approximation, corrections to conductivity and the vortex lattice energy dissipation from higher Landau levels are systematically calculated and compared to a recent experiment.

DOI: 10.1103/PhysRevB.70.214529 PACS number(s): 74.40.+k, 74.25.Ha, 74.25.Dw

I. INTRODUCTION

The static Abrikosov flux lattice has been experimentally observed since the 1960s by a great variety of techniques and lateral correlations have been clearly observed recently up to tens of thousands of lattice spacings.[1] The remarkable advances in decoration, small-angle neutron scattering, and muon spin rotation techniques allowed a recently direct glimpse into the structure of the moving Abrikosov vortex systems.[2–5] It shows that at small flux flow velocities vortices move in channels as predicted in Ref. 7. When the flux flow velocity increases beyond the one corresponding to the critical current, one observes a relatively well correlated hexagonal lattice. The channels and the plastic flow at relatively low velocities are explained by the influence of pinning on the basis of theoretical arguments[8] and confirmed by numerous simulations.[8–12] At high velocity of the moving lattice (corresponding to the high electric field), the influence of disorder is expected to diminish and a "moving Bragg glass" appears.[8,13] Indeed Bragg peaks roughly at positions of the hexagonal lattice were observed[5] recently.

Since the theoretical prediction of the moving Bragg glass exhibiting the transverse peak effect,[13] much effort has been put into the simulation of the high driving force phase of the moving vortex system.[10–12] In particular it was found[10] that as the driving force increases (or disorder decreases) the vortex lattice suddenly changes orientation for a period of time and then returns to a "regular" drift mode. The main emphasis in these studies mentioned above is still the effects of pinning on the moving lattice.

Experiments at a low (below 100 G) magnetic field and slow flux moving velocity (of order μm/s) showed that the orientation of the moving vortex lattice is tied to the direction of motion, namely, when a nearly hexagonal lattice is observed, one always observes the orientation depicted in Fig. 1(a), never the "rotated" one of Fig. 1(b).[4] Here the effect of pinning cannot be ignored and plays an important role in the orientation of the vortex lattice. However, the most recent small-angle neutron scattering and muon spin

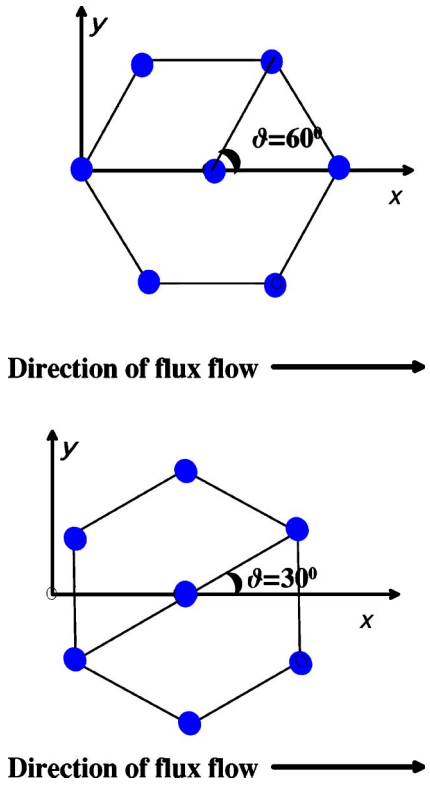

FIG. 1. Two possible orientations of the (approximately) hexagonal vortex lattice. (a) The direction of the flux lines is the same as the nearest neighbors lattice orientation. (b) The direction of the flux lines is perpendicular to the nearest neighbors lattice orientation.

rotation experiment can probe the moving lattice at much higher velocities of order cm/s or even higher. The results about the orientation of the moving lattice obtained in Ref. 5 seem to be different from the case at a low magnetic field and slow flux moving velocity.

The effect of pinning is expected to be smaller at higher velocities. Alternatively one can ask what happens in very clean materials. A recent experiment in Pn-In seems to belong to this category.[5] As the pinning influence diminishes with increasing flux velocity, it is natural to ask what would happen in the limit of the highest possible flux velocity (of course, eventually the electric field destroys superconductivity, so that the mathematical limit of the infinite driving force is unphysical) disregarding pinning altogether.

The question of the orientation of the vortex lattice usually does not arise in the static case. Without an external electric field singling out a particular direction one has a complete degeneracy of possible orientations of the hexagonal vortex lattice. This is not surprising for a sufficiently symmetric material (like $NbSe_2$ frequently used in experiments belongs to this category): the rotational symmetry ensures that the free energy is independent of the hexagonal lattice orientation. The rotational symmetry is broken by the motion of fluxons as was confirmed experimentally.[4,6] Naturally one could ask whether the particular lattice orientation observed for example in Ref. 4 is necessarily tied to pinning or might appear in clean superconductors as well. Furthermore, the lattice also can be deformed though the deformation apparently is very small [see Figs. 1(c) and 1(d) in Ref. 4]. Is there a deformation even before pinning centers disorder the lattice?

It would be difficult to address the question of the moving vortex lattice structure using phenomenological models like the elastic medium[13] (in which individual vortices are simply not "seen") or approximating vortices in the London approximation by interacting lines or points r_i in two dimensions (2D).[12] To give an example of the problems in the London limit, let us consider equations of motion for vortices. The driving force **F** is the Lorentz force and the dynamics is assumed overdamped:

$$\eta\frac{d\mathbf{r}_i}{dt} = -\sum_{j\neq i}\nabla U(\mathbf{r}_i-\mathbf{r}_j)+\mathbf{F}, \tag{1}$$

where $U(\mathbf{r}_i-\mathbf{r}_j)$ is the intervortex repulsive potential. The solution of these equations in the absence of pinning is obvious: the "boosted" hexagonal lattice of any orientation irrespective of the direction of **F**. Thus the orientation of the lattice depends solely on initial conditions, at least in the clean case. Therefore the approximations made in the above phenomenological approaches are too strong.

In this paper we use the time-dependent Ginzburg-Landau (TDGL) model to study the vortex motion and structure. The TDGL approach has been remarkably successful in describing various thermodynamical and transport properties.[14] Progress in obtaining the theoretical results from the model can be achieved only when certain additional assumptions are made. One of the often made additional assumption is that only the lowest Landau level (LLL) significantly contributes to physical quantities of interest. The LLL approximation is valid for $H>H_{c2}(T)/13$ in the static limit.[15] Although most of the experiments concerning a moving lattice were performed at a field far below the static $H_{c2}(T)$, it has been shown a long time ago[16,17] that in the presence of electric field E the effective $H_{c2}(T,E)=H_{c2}(T)-\gamma^2V^2\Phi_0/(8\pi)$ where $V=cE/B$ is the velocity of fluxons and γ is the inverse diffusion constant setting the time scale in the TDGL approach. This field $H_{c2}(T,E)$ could be much smaller at not very small fluxon velocities (electric field suppresses superconductivity even more effectively than the magnetic field). Therefore effectively one can move into the region of validity of the LLL approximation at sufficiently large currents. Moreover, one expects that, even beyond the region of validity of the LLL approximation, physics is qualitatively the same.

We solve TDGL equations for a moving vortex solid without disorder and find the vortex structure to which the moving lattice relaxes irrespective of initial conditions.[16–18] It turns out that the preferred lattice is rhombic. The distortion is velocity dependent. Remarkably the orientation is the same as in Fig. 1(a); namely, it agrees with experiments only at velocities exceeding the critical one (of order of cm/s for superconducting type II low T_c metals). Below it the orientation is rotated by 30°.

The paper is organized as follows. The model is described, symmetries analyzed, and the perturbative mean field solution developed in Sec. II. The general formalism is developed to treat the non-Hermitian part of the equation. The shape and the orientation of the vortex lattice and the reorientation transition are described in Sec. III. Then in Sec. IV we calculate corrections due to higher Landau levels and derive a general expression for conductivity. It is compared with a recent experiment. Section V is a summary.

II. MODEL AND ITS PERTURBATIVE FLUX FLOW SOLUTION

A. Time-dependent GL model

Our starting point is the TDGL equation,[19]

$$\frac{\hbar^2\gamma}{2m_{ab}}\left(\frac{\partial}{\partial t}+\frac{ie^*}{\hbar}\Phi\right)\psi=-\frac{\delta}{\delta\psi^*}F. \tag{2}$$

The static GL free energy is

$$F=\int d^3x\left(\frac{\hbar^2}{2m_{ab}}\left|\left(\vec{\nabla}+\frac{ie^*}{\hbar c}\vec{A}\right)\psi\right|^2+\frac{\hbar^2}{2m_c}|\partial_z\psi|^2-\alpha(T_c-T)\times|\psi|^2+\frac{b'}{2}|\psi|^4\right), \tag{3}$$

where α and b' are phenomenological parameters, γ is the inverse diffusion constant which controls the scale of dynamical processes via dissipation. As usual the magnetic induction is $\vec{B}=\vec{\nabla}\times\vec{A}$ and electric field $\vec{E}=-\vec{\nabla}\Phi-(\partial/\partial t)\vec{A}$. It should be supplemented by Ampere's law[17,18]

$$\vec{\nabla} \times \vec{B} = \sigma_n \vec{E} + \vec{J}_s, \tag{4}$$

where the first term is the contribution of the normal liquid in the framework of the two liquid model and the second term is the supercurrent

$$\vec{J}_s = -\frac{i\hbar e^*}{2m}\psi^* \left(\vec{\nabla} + \frac{ie^*}{\hbar c}\vec{A}\right)\psi + \text{c.c.} \tag{5}$$

Tensor σ_n is the normal state conductivity. We assume that the coefficient of the covariant time derivative term γ in Eq. (2) is real although a small imaginary (Hall) part is always present.[18] The general case will be discussed in Sec. V.

We make several approximations (identical to those made in Ref. 20 and major parts of Ref. 17) so that the problem becomes manageable. The physical conditions allowing those approximations are the following. Temperatures and magnetic fields are close "enough" to $H_{c2}(T)$. Under this assumption the order parameter ψ is suppressed compared to its Meissner value. In this paper we will also assume strongly type II superconductivity $\kappa = \lambda/\xi \gg 1$ [$\xi^2 = \hbar^2/(2m_{ab}\alpha T_c)$, $\lambda^2 = c^2 m^* b'/4\pi e^{*2}\alpha T_c$]. The magnetic field is very homogeneous since the vortices overlap. The characteristic length describing the inhomogeneity of the electric field was identified in Ref. 17: $\zeta^2 = (4\pi\sigma_n/\gamma)\lambda^2$ and since typically $\sigma_n \simeq \gamma$, thus $\zeta \gg \xi$ and the electric field is assumed homogeneous. Therefore the Maxwell type equations for the electromagnetic field are not considered. The time-independent vector potential will be taken in Landau gauge $\vec{A} = (By, 0, 0)$ and describes a nonfluctuating magnetic field in the direction $-\hat{z}$. The scalar potential is also independent of time $A_0 = Ey$ and describes the electric field oriented along the negative y axis. The vortices are therefore moving along the x direction. We neglect thermal fluctuations and disorder on the mesoscopic scale.

Throughout most of the paper we will use the following physical units. The unit of length is the coherence length ξ, the unit of the magnetic field is $H_{c2} = \Phi_0/2\pi\xi^2$, $\lambda = (c/e^*)\sqrt{m_{ab}b'/4\pi\alpha T_c}$, and the unit of energy (temperature) is T_c. In these units the magnetic field is denoted by $b \equiv B/H_{c2}$. The asymmetry of masses between the z direction and the x-y plane can be removed by rescaling coordinates and time: $x \to \xi x/\sqrt{b}$, $y \to \xi y/\sqrt{b}$, $z \to \xi z/\sqrt{b m_c/m_{ab}}$, $t \to (\gamma\xi^2/2b)t$. The TDGL equations, after the order parameter field is rescaled as well $\psi \to \sqrt{2\alpha T_c b/b'}\psi$, are

$$\begin{aligned} 0 &= L\psi + \psi|\psi|^2, \\ L &\equiv D_t - \tfrac{1}{2}[D_x^2 + \partial_y^2 + \partial_z^2] - a, \end{aligned} \tag{6}$$

where $a \equiv (1 - T/T_c/2b)$, $v = (c\gamma E/2B)\sqrt{\hbar c/e^* B}$ is scaled vortex velocity (in units of $2\sqrt{2\pi B/\Phi_0}/\gamma$), and covariant derivatives are defined by $D_x = \partial/\partial x - iy$ and $D_t = \partial/\partial t + ivy$. Since ∂_z^2 commutes with L, the equations are invariant under the z translations, the z dependence of the solutions decouples and is generally a plane wave. It is easy to see that the relevant solution does not break this symmetry and is therefore constant with respect to z. Consequently we consider the problem as a 2+1-dimensional one [note, however, that if the three-dimensional (3D) disorder or thermal fluctuations are included one cannot ignore the z coordinate as the configuration of disorder can destroy the translational symmetry along the z direction].

B. Expansion of a nontrivial solution around dynamical phase transition point

The line in parameter space (a, v), which separates the normal region in which the only solution is $\psi = 0$ from the flux flow nontrivial solution region, has been found by Hu and Thompson.[17] We will construct a perturbative solution of the TDGL equations near the mixed state–normal phase transition line analogous to the one in statics.[21] The range of applicability and precision of the LLL approximation at large κ in statics was explored recently.[15] The main difficulty in the dynamical case is that the linear part of the equation L is not Hermitian due to the dissipation term D_t.

A general idea of the expansion around a bifurcation point of a nonlinear equation is as follows. One looks for a set of eigenfunctions of the linear part of Eq. (6):

$$L_{Np\omega}\phi = \Theta_{Np\omega}\phi_{Np\omega}. \tag{7}$$

The operator L consists of two parts: the usual Hermitian Hamiltonian of a particle in magnetic field $-\frac{1}{2}[D_x^2 + \partial_y^2]$ and the anti-Hermitian covariant time derivative D_t. The complete set of eigenfunctions with "quantum" numbers N and $p_x \equiv p$ is

$$\begin{aligned} \phi_{Np\omega} &= \frac{1}{\sqrt{\pi 2^N N!}} \\ &\quad \times \exp[i(px - \omega t)] H_N(y - p + iv) \\ &\quad \times \exp\left[-\frac{1}{2}(y - p + iv)^2\right], \\ \Theta_{Np\omega} &= -a + N + \frac{1}{2} + \frac{v^2}{2} - i(\omega - vp), \end{aligned} \tag{8}$$

where H_N are Hermitian polynomials. Unlike the usual case of a Hermitian operator, eigenfunctions and eigenvalues of the Hermitian conjugate of the operator $L^\dagger$ are different:

$$L^\dagger \phi_{Np\omega} = \Theta_{Np\omega}\phi_{Np\omega},$$

$$\begin{aligned} \overline{\phi}_{Np\omega} &= \frac{1}{\sqrt{\pi 2^N N!}} \exp[-i(px - \omega t)] H_N(y - p + iv) \\ &\quad \times \exp\left[-\frac{1}{2}(y - p + iv)^2\right], \\ \overline{\Theta}_{Np\omega} &= -a + N + \frac{1}{2} + \frac{v^2}{2} + i(\omega - vp). \end{aligned} \tag{9}$$

Note that $\overline{\phi}$ is not a complex conjugate of ϕ. The orthogonality relations in the dynamical case involve both $\phi_{Np\omega}$ and $\overline{\phi}_{Np\omega}$:

$$\int_{x,y,t} \bar{\phi}_{Np\omega}(x,y,t)\phi_{N'p'\omega'}(x,y,t) = (2\pi)^2 \delta_{NN'}\delta(p-p') \times \delta(\omega-\omega'), \quad (10)$$

$$\langle \bar{\phi}_{Np\omega}(x,y,t)\phi_{Np\omega}(x,y,t)\rangle_{x,y,t} = 1,$$

where the averaging over space and time is denoted by $\langle\cdots\rangle_{x,y,t}$.

The bifurcation (in this case the dynamical transition) occurs when there exists a set of eigenfunctions of L' with zero eigenvalues $\Theta_{Np\omega}=0$:

$$a_{bif}(v) = N + \frac{1}{2} + \frac{v^2}{2}, \quad (11)$$

$$\omega = vp. \quad (12)$$

It is clear that solutions with $N>0$ are unstable as in the static case.[19] Equation (11) with $N=0$ gives the phase transition line of Ref. 17, while Eq. (12) selects the "zero manifold" in the space of functions. We define the "distance" from the transition line

$$a_h(v) \equiv a - a_{bif}(v) = a - \frac{1}{2} - \frac{v^2}{2}. \quad (13)$$

When $a_h(v)>0$, the nonlinear TDGL equation,

$$L\psi + \psi|\psi|^2 \equiv L_{sh}\psi - a_h(v)\psi + \psi|\psi|^2 = 0, \quad (14)$$

$$L_{sh} = L + a_h(v),$$

is solved perturbatively in a_h with a nonanalytic prefactor, as in the static case:

$$\Phi = [a_h(v)]^{1/2}[\Phi^0 + a_h\Phi^1 + \cdots]. \quad (15)$$

To order $[a_h]^{1/2}$, the equation linearizes

$$L_{sh}\Phi^0 = 0. \quad (16)$$

Therefore Φ_0 belongs to the "zero manifold" and thereby can be expanded,

$$\Phi^0 = \sum_p c_p\phi_{N=0,p,\omega=vp} \equiv \sum_p c_p\phi_p, \quad (17)$$

with coefficients c_p determined by the next order equation. As a result, since all the $\phi_p(x,y,t)$ depend only on the combination $px-\omega t=p(x-vt)$ rather than separately on x and t, vortices move in the direction perpendicular to both the electric and the magnetic field with constant velocity v. To order $[a_h]^{3/2}$, one obtains

$$L_{sh}\Phi^1 = \Phi^0 - \Phi^0|\Phi^0|^2.$$

Multiplying this equation by $\bar{\phi}_p$ and integrating over (x,y,t) using the orthogonality relation, Eq. (10), one obtains the following infinite set of nonlinear algebraic equations:

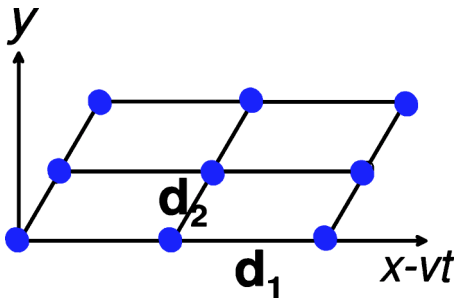

FIG. 2. The flux lattice geometry: $\mathbf{d}^{(1)}$, $\mathbf{d}^{(2)}$ are the translational symmetry vectors which determines the primitive cell of the flux lattice. The angle between these two vectors is θ.

$$\sum_{p_1,p_2,r} c_{p_1}c_{p_2}c_r^*\langle\bar{\phi}_p\phi_r^*\phi_{p_1}\phi_{p_2}\rangle_{x,y,t} = c_p. \quad (18)$$

We will study the solution of this set in the next section.

III. SHAPE AND ORIENTATION OF THE MOVING LATTICE

A. Symmetry and energetics considerations

It is well known in the static case that there is a solution of GL equations for any lattice symmetry. The same is true in the dynamical case as well, but the symmetries should take into account the motion of vortices. We define the covariant derivatives in a matrix 2+1-dimensional form (a summation over repeated indices assumed),

$$A_\mu = b_{\mu\nu}x_\nu, \quad D_\mu = \partial_\mu - iA_\mu, \quad (19)$$

and the Landau gauge

$$b_{\mu\nu} = \begin{pmatrix} 0 & 1 & 0 \\ 0 & 0 & 0 \\ 0 & -v & 0 \end{pmatrix} \quad (20)$$

is used in our paper. All indices run over space $\mu=1(x)$, $2(y)$, and $3(t)$. The electromagnetic translation operators satisfying $[T_d, D_\mu]=0$ are

$$T_d = e^{i\mathbf{d}\cdot\mathbf{P}} = \exp\left[-i\left(\frac{1}{2}d_\mu b_{\mu\nu}d_\nu + x_\nu b_{\nu\mu}d_\mu\right)\right]e^{i\mathbf{d}\cdot\mathbf{p}}, \quad (21)$$

where generators are $P_\mu=-i(\partial_\mu - ib_{\nu\mu}x_\nu)$ (note a transpose in the matrix $b_{\mu\nu}$). Operators $p_\mu=-i\partial_\mu$ are usual (not "electromagnetic") translation operators. The following commutation relations:

$$[P_\mu, P_\nu] = i(b_{\mu\nu} - b_{\nu\mu}), \quad (22)$$

can be verified. Thus we will have $[i\mathbf{d}_1\cdot\mathbf{P}, i\mathbf{d}_2\cdot\mathbf{P}] = -id_{1\alpha}d_{2\beta}(b_{\alpha\beta}-b_{\beta\alpha})$. Using the Haussdorf formula one checks that the electromagnetic translation operators obey $e^{i\mathbf{d}_1\cdot\mathbf{P}}e^{i\mathbf{d}_2\cdot\mathbf{P}} = e^{i\mathbf{d}_2\cdot\mathbf{P}}e^{i\mathbf{d}_1\cdot\mathbf{P}}e^{[i\mathbf{d}_1\cdot\mathbf{P},\ i\mathbf{d}_2\cdot\mathbf{P}]}$. (See Fig. 2.) If $\mathbf{d}_1$ and $\mathbf{d}_2$ are the lattice vectors which preserve the symmetry of the system (when one translates the system by $\mathbf{d}_1$ or $\mathbf{d}_2$, the system will be unchanged), one shall require $e^{i\mathbf{d}_1\cdot\mathbf{P}}\psi = e^{i\mathbf{d}_2\cdot\mathbf{P}}\psi$ and it will lead to

$$e^{i\mathbf{d}_1\cdot\mathbf{P}}e^{i\mathbf{d}_2\cdot\mathbf{P}}\psi = e^{i\mathbf{d}_2\cdot\mathbf{P}}e^{i\mathbf{d}_1\cdot\mathbf{P}}e^{[i\mathbf{d}_1\cdot\mathbf{P},\ i\mathbf{d}_2\cdot\mathbf{P}]}\psi = e^{[i\mathbf{d}_1\cdot\mathbf{P},\ i\mathbf{d}_2\cdot\mathbf{P}]}\psi = \psi.$$

Therefore we should demand

$$[i\mathbf{d}_1\cdot\mathbf{P},\ i\mathbf{d}_2\cdot\mathbf{P}] = i2\pi\times\text{integer}.$$

This requirement is satisfied by the following basic translation symmetry vectors:

$$\mathbf{d}^{(1)} = a_\Delta\left(\frac{1}{2},0,-\frac{1}{2v}\right),$$

$$\mathbf{d}^{(2)} = a_\Delta\left(\frac{r}{2},r',-\frac{r}{2v}\right), \tag{23}$$

$$\mathbf{d}^{(0)} = \tau(v,0,1).$$

Here a_Δ is the lattice spacing along the direction of motion, τ is arbitrary (a continuous translational symmetry). The flux quantization (one flux quantum per unit cell assumed) determines r': $r'a_\Delta^2=2\pi$. The $\mathbf{d}^{(1)}$ translation symmetry leads to the discrete parameter

$$p = \frac{2\pi}{a_\Delta}l \equiv gl,$$

in Eq. (17), and the set of equations, Eq. (18), will take a form

$$c_n = \sqrt{\frac{1}{2}}g^2\sum_{l_1,l_2} c_{l_1+n}c_{l_2+n}c^*_{l_1+l_2+n} \times\exp\left\{-\frac{1}{2}[(gl_1+iv)^2+(gl_2+iv)^2-v^2]\right\}. \tag{24}$$

It can be solved as in the static case by an Ansatz

$$c_l = \sqrt{\frac{g}{\sqrt{\pi}\beta_A(v)}}e^{-i\pi rl(l+1)},$$

with the Abrikosov function

$$\beta_A(v) = \frac{g}{\sqrt{2\pi}}\sum_{l1,l2} \times\exp\{2\pi irl_1l_2\} \times\exp\left\{-\frac{1}{2}[(gl_1+iv)^2+(gl_2+iv)^2-v^2]\right\}. \tag{25}$$

Consequently,

$$\Phi^0(x,y,z) = \frac{1}{\sqrt{\beta_A(v)}}\varphi(x,y), \tag{26}$$

where

$$\varphi(x,y) \equiv \sqrt{\frac{g}{\sqrt{\pi}}}\sum_l \exp\{il[g(x-vt)-\pi r(l+1)]\} \times\exp\left[-\frac{1}{2}(y-gl-iv)^2\right] \tag{27}$$

is normalized by $\langle|\varphi|^2\rangle_{x,y}=1$.

In the static case a solution which has minimal free energy is physically realized. The free energy is proportional to $-[a_h(0)]^2/[2\beta_A(0)]$ which therefore should be minimized. This means that one should minimize $\beta_A(0)$. The minimal $\beta_A(0)=1.16$ is obtained for the hexagonal lattice. Similar reasoning cannot be applied to the moving lattice solution of the TDGL equation since the friction force is nonconservative. Under these circumstances Ketterson and Song[22] calculated the work made by the friction force:

$$S \equiv \frac{d}{dt}S = 2\gamma\langle|D_t\psi|^2\rangle_{x,y}. \tag{28}$$

The preferred lattice structure in the steady state corresponds to a state with largest $\dot{S}$. For the lattice solution of the TDGL equation one obtains to leading order in α_h,

$$\dot{S} \propto \frac{g|\alpha_h(v)|}{\beta_A(v)}\left\langle\left|\sum_l\left(\frac{\partial}{\partial t}+ivy\right)\exp\{il[g(x-vt) - \pi r(l+1)]\}\exp\left[-\frac{1}{2}(y-gl-iv)^2\right]\right|^2\right\rangle_{x,y} = \frac{v^2|\alpha_h(v)|}{2\beta_A(v)}e^{v^2}. \tag{29}$$

We therefore shall minimize β_A as function of r and a_Δ. This is consistent with the static case.

B. The stationary orientation of the flux lattice. The reorientation transition at high flux flow velocity

We found that the minimum of $\beta_A(v)$ always appears when $r=1/2$, namely for rhombic lattices. Therefore from now on we consider these lattices only. As a function of an angle of the rhombic lattice $\tan\theta=4\pi/a_\Delta^2$ (see Fig. 1 for a definition of θ) it generally has two minima; see Fig. 3. In the static case the two minima are degenerate with $\theta=60°$, 30° corresponding to perpendicular orientations of the hexagonal lattice, while for nonzero velocity the degeneracy is lifted. Note that originally[16,17] it was assumed that the lattice is hexagonal also in the dynamical case. Generally the shape is not strongly distorted for physically realizable velocities. For velocities smaller than $v_c=0.95$ angle θ close to 60° [the orientation of Fig. 1(b)] is preferred over the one close to 30° [the orientation of Fig. 1(a)]; see Fig. 3(c). The dependence of the angle θ on velocity can be very well fitted in the whole range $v<0.5$ by

$$\theta = 30 - 0.4v - 24v^2. \tag{30}$$

The Abrikosov function also depends on velocity increasing according to

$$\beta_A(v) = \beta_A(0)(1+1.25v^2), \tag{31}$$

where $\beta_A(0)=1.1596$ is the static value for a hexagonal lattice. As the critical velocity is approached the two minima coincide; see Fig. 3(b). Beyond that point the preferred structure is just the opposite; Fig. 3(a). The transition is first order and the coexistence region should exist.

We now make a few comments about the orientation of the lattice. The reader might have noticed that the orientation

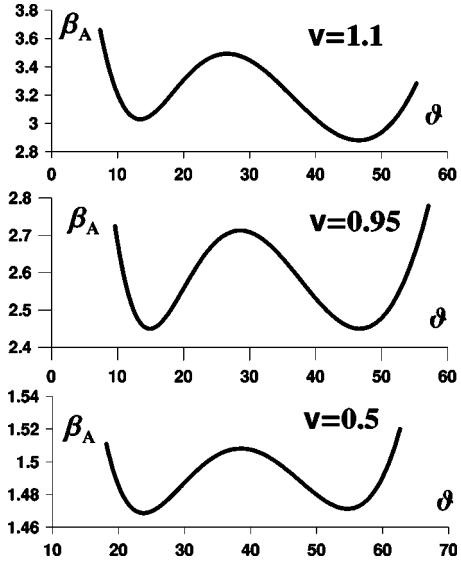

FIG. 3. The dependence of the Abrikosov β parameter on orientation and shape of the vortex lattice moving with scaled velocities $v=0.5,0.95,1.1$. The angle θ is defined as an angle between the direction of motion and a crystallographic axis in the direction of the symmetry transformation d_2. The minimum favors the smaller angle close to 30° corresponding to the structure of Fig. 1(a) for $v<v_c$, while the other local minimum corresponding to Fig. 1(b) (angles close to 60°) is preferred for $v>v_c$.

of the lattice is not completely arbitrary since the direction of the vector $\mathbf{d}_1$ coincides with the direction of the vortex motion. The most general $\beta_A(v)$ is given by Eq. (25) with arbitrary r. We minimized numerically the Abrikosov β function and found that the solution with the largest dissipation is always of the more symmetric type $r=1/2$. One can argue that despite the fact that the electric field breaks the continuous rotational symmetry, it still preserves a discrete transformation $y\to -y$, $\psi\to\psi^*$. The solution $r=1/2$ preserves this discrete symmetry. This symmetry is unlikely to be spontaneously broken. Indeed the symmetry was observed in the experiments (for example, in Ref. 4).

IV. NONLINEAR CONDUCTIVITY AND BREAKDOWN OF THE LLL SCALING IN TRANSPORT

In this section we first calculate the leading higher Landau level corrections to the solution of the TDGL equation, Eq. (6). Then we use it to derive the correction to the LLL scaling of conductivity.[18,20,23]

A. Higher orders in a_h correction to the moving lattice solution

Using the same symmetry arguments as for the leading order, the second term in Eq. (15) can be expanded as

$$\Phi^1=\sum_{N=0} C_N^1\varphi_N, \tag{32}$$

$$\varphi_N=\sqrt{\frac{g}{\sqrt{\pi}2^N N!}}\sum_l \exp\{il[g(x-vt)-\pi r(l+1)]\}$$
$$\times H_N(y-gl-iv)\exp\left[-\frac{1}{2}(y-Gl-iv)^2\right].$$

Multiplying Eq. (14) by $\overline{\varphi_N}$ for $N>0$, one obtains

$$NC_N^1=-\beta_A^{-3/2}\langle\overline{\varphi_N}\varphi^*\varphi\varphi\rangle. \tag{33}$$

To find C_0^1 we need in addition also the order $a_h^{5/2}$ equation:

$$L_{sh}\Phi^2=\Phi^1-(2\Phi^1|\Phi^0|^2+\Phi^{1*}\Phi^0\Phi^0). \tag{34}$$

The inner product with φ gives

$$NC_0^1=-\beta_A^{-5/2}\sum_{N=1}^{\infty}[2\langle\overline{\varphi_N}\varphi^*\varphi\varphi\rangle\langle\overline{\varphi}\varphi^*\varphi_N\varphi\rangle+\langle\overline{\varphi_N^*}\varphi^*\varphi^*\varphi\rangle$$
$$\times\langle\overline{\varphi}\varphi_N^*\varphi\varphi\rangle]. \tag{35}$$

Note that for the hexagonal lattice, $\langle\overline{\varphi_N}\varphi^*\varphi\varphi\rangle\neq 0$ only when $N=6j$, where j is an integer. This is due to hexagonal symmetry of the vortex lattice.[21] In statics $\beta_N=\langle\overline{\varphi_N}\varphi^*\varphi\varphi\rangle$ decreases very fast with j: $\beta_6=-0.2787$, $\beta_{12}=0.0249$.[15] Because of this the coefficient of the next to leading order is very small (also an additional factor of 6 in the denominator helps the convergency).

B. The LLL scaling in nonlinear conductivity

In the flux flow regime, in addition to the normal state conductivity, there is a large contribution from the Cooper pairs represented by the order parameter field. It was noted in Refs. 18, 20, and 23 that the LLL contribution to nonlinear conductivity,

$$\sigma=-\frac{i\hbar e^*}{2mE}\psi^*\left(\vec{\nabla}+\frac{ie^*}{\hbar c}\vec{A}\right)\psi, \tag{36}$$

is proportional to the superfluid density. The scaled dimensionless conductivity is defined as $\sigma_{scaled}\equiv(4\pi\kappa^2/c^2\gamma)\sigma$ and σ_{scaled} in the LLL approximation is

$$\sigma_{LLL}=\frac{i}{2v}\langle\Psi_{LLL}^*\partial_y\Psi_{LLL}-\Psi_{LLL}\partial_y\Psi_{LLL}^*\rangle=\langle|\Psi_{LLL}|^2\rangle. \tag{37}$$

The last equality is due to the general property of the LLL functions; see Eq. (8). It follows the naive expectation of a "Drude"-like formula[19] with $|\Psi_{LLL}|^2$ playing a role of "charge carriers" density (meaning here Cooper pairs).

To leading order in a_h using the results of Sec. II one gets

$$\sigma_{LLL}=\frac{ia_h(v)}{2\beta_A(v)v}\langle\varphi^*\partial_y\varphi-\varphi\partial_y\varphi^*\rangle=\frac{a_h(v)}{\beta_A(v)}e^{v^2}, \tag{38}$$

where $a_h(v)=(1-t_{GL}-b-v^2)/(2b)$. At finite v there is an exponential factor coming from the nonorthogonality of eigenfunctions of a non-Hermitian operator and, in addition, similar dependence in β_A and quadratic in a_h. In the limit $v\to 0$ one recovers the Ohmic expression (see Ref. 18) returning to standard units,

$$\sigma_{LLL}^{(1)} = \sigma_0 \frac{1 - t_{GL} - b}{2b\beta_A(0)}, \quad \sigma_0 \equiv \frac{c^2\gamma}{4\pi\kappa^2}, \tag{39}$$

while the leading nonlinear (cubic) correction is, using Eq. (31),

$$\sigma_{LLL}^{(3)} = \sigma_0 \frac{t_{GL} + b - 5}{8b\beta_A(0)} v^2, \tag{40}$$

where $v = (c\gamma E/2B)\sqrt{\hbar c/e^* B}$.

C. Leading correction to the LLL scaling

Generally to all orders in a_h one can write $\Psi = \Sigma_N C_N(a_h)\varphi_N$,

$$\sigma = \sigma_0 \frac{i}{2v} \sum_{NM} C_N^*(a_h) C_M(a_h) \langle \varphi_N^* \partial_y \varphi_M - \varphi_M \partial_y \varphi_N^* \rangle$$
$$\equiv \sigma_0 \sum_{NM} C_N^*(a_h) C_M(a_h) \sigma_{NM}. \tag{41}$$

For $N > M$ and $N-M$ even integer,

$$\sigma_{NM} = -\sqrt{\frac{2^{N-M} M!}{N!}} (-v^2)^{(N-M)/2} \left[v^2 L_{M-1}^{N-M+1}(-2v^2) + \frac{M+1}{2} L_{M+1}^{N-M-1}(-2v^2) \right] e^{v^2}, \tag{42}$$

where $L(y)$ are Laguerre polynomials. This contribution is always sub-Ohmic $\sigma_{NM} \sim v^{N-M}$ at small v. If $N-M$ is odd, the contribution vanishes. The diagonal contributions are simpler,

$$\sigma_{NN} = [L_{N-1}^1(-2v^2) + L_N^1(-2v^2)] e^{v^2}, \tag{43}$$

and have an Ohmic part,

$$\sigma_{NN} = 2N + 1.$$

The first term, proportional to Landau orbital number N, is responsible for the breaking of the naive Drude-like expectation that conductivity is proportional to $|\Psi|^2$.[19] One observes that higher Landau levels contribute to conductivity more than to $|\Psi|^2$. One can interpret this as an "increased charge movers density."

Thus the Ohmic conductivity has two contributions,

$$\sigma^{(1)} = \sigma_0 \sum_N (2N+1) |C_N(a_h)|^2 = \sigma_1 + \sigma_2, \tag{44}$$

$$\sigma_1 = \sigma_0 \langle |\Psi|^2 \rangle, \quad \sigma_2 = 2\sigma_0 \sum_{N=1} N |C_N(a_h)|^2, \tag{45}$$

the first proportional to the superfluid density, while the second, the HLL part, is not and is of order a_h^3 only. Substituting expressions for C_0 from the previous section, we obtain for the Ohmic conductivity to order a_h^2,

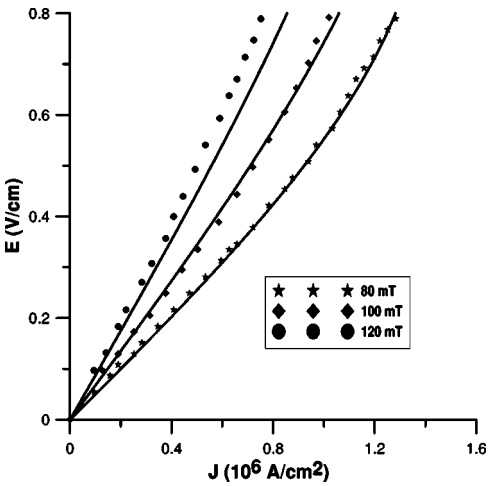

FIG. 4. Current-voltage curves at high flux flow velocities. The data of Ref. 24 on Nb films at $T = 7.8$ K (symbols represent different magnetic fields) are compared with theory combining the linear (Ohmic) contribution Eq. (46), and the cubic correction, Eq. (40).

$$\sigma_1 = \sigma_0 \left[\frac{a_h}{\beta_A} + 3 \frac{a_h^2}{\beta_A^3} \sum_{N=1} \frac{\beta_N^2}{N} \right], \tag{46}$$

where all the quantities are taken in the limit $v \to 0$. The sum rapidly converges in the static (or low velocity) case: $\Sigma_N(\beta_N^2/N) = 0.0131$.

D. Comparison with experiment

In Fig. 4 we compare the results with recent experiments at high currents (electric fields) of Ref. 24 on Nb in which vortex velocities are as high as 10^5 cm/s. We used the same values of the Ginzburg-Landau parameter $\kappa = 9.4$ and the inverse diffusion constant $\gamma = 1.17$ s/cm^2 to fit all three curves corresponding to magnetic fields $H = 80$ mT, 100 mT, and 120 mT for a "cold" sample with $T_c = 8.6$ K. We used the measured (inset in Fig. 2 of Ref. 24) $H_{c2} \equiv T_c [dH_{c2}(T)/dT]|_{T=T_c} = 4.4$ T. The temperature was $T = 7.8$ K close enough to T_c so that the a_h^2 correction was always below 10%. The value of parameter γ is in good agreement the measured normal state resistivity of 9.9 $\mu\Omega$ cm. The results agree well with the flux flow Ohmic conductivity data at relatively low currents (still well above the critical current) exhibiting the $1/H$ behavior presented in Fig. 2 of Ref. 24.

One observes that the full expression (solid lines) is closer to the experiment at very high electric fields. Several curves for the magnetic field are given. The smallest is clearly off the LLL approach range.

V. CONCLUSION

To summarize, we have considered the dynamics of the vortex lattice, neglecting the effects of pinning. We studied the time-dependent Ginzburg-Landau equation in the lowest Landau level approximation. For the validity region of the LLL approximation, as in the static case, we require $a_h = (1/2B)[H_{c2}(T) - B - (c^2\gamma^2\Phi_0 E^2/4\pi B^2)] \ll 6$, the factor 6

coming from cancellations of the higher Landau level effects due to hexagonal symmetry (even the hexagonal symmetry is approximate in the moving lattice). We systematically calculated higher Landau level corrections to conductivity and the vortex lattice energy dissipation. The stationary lattice structure depends on the flux flow velocity. While for small velocities $V<2v_c\sqrt{2\pi B/\Phi_0}/\gamma$, the $v_c=0.95$ vortex lattice is oriented as in Fig. 1(b), while beyond this velocity orients as in Fig. 1(a). We emphasize that in our calculation the pinning effect was disregarded. Of course, as was firmly established in numerous theoretical and experimental investigations, pinning significantly can modify the picture for low velocities. Pinning generally "prefers" the configuration of Fig. 1(a) and this is a possible reason why the experimental observed orientation is depicted as in Fig. 1(a). However one can expect that for higher velocities and very clean samples the pinning dominated dynamics crosses over into the interactions dominated dynamics considered in the present work. The high velocity of order cm/s is unlikely to be seen in decoration experiments. However other techniques like SANS and muon spin rotation[5] and possibly Lorentz microscopy[25] are able to detect the lattice structure even at such relatively high velocities. At very high velocities the results for nonlinear conductivity agree with recent experiments[24].

ACKNOWLEDGMENTS

We are especially grateful to F. P. Lin for fitting the conductivity data. We are grateful to E. Andrei, A. Knigavko, T. J. Yang, A. Shaulov, Y. Yeshurun for a discussion, and E. M. Forgan for a discussion and sending results prior to publication. The work of A.M. was supported by the graduate students program of NCTS. The work of B.R. was supported by the NSC of the R.O.C., NSC No. 932112M009024 and the hospitality of Peking University. The work of D.L. was supported by the Ministry of Science and Technology of China (Grant No. G1999064602) and the National Natural Science Foundation of China (Grant No. 10274030).

[1] P. Kim, Z. Yao, C. A. Bolle, and C. M. Lieber, Phys. Rev. B **60**, R12589 (1999).
[2] U. Yaron *et al.*, Phys. Rev. Lett. **73**, 2748 (1994).
[3] M. Marchevsky, J. Aarts, P. Kes, and M. Indenbom, Phys. Rev. Lett. **78**, 531 (1997).
[4] F. Pardo, F. de la Cruz, P. L. Gammel, E. Bucher, and D. J. Bishop, Nature (London) **396**, 348 (1998).
[5] D. Charalambous, P. G. Kealey, E. M. Forgan, T. M. Riseman, M. W. Long, C. Goupil, R. Khasanov, D. Fort, P. J. C. King, S. L. Lee, and F. Ogrin, Phys. Rev. B **66**, 054506 (2002).
[6] E. Andrei (private communication).
[7] L. Balents, M. C. Marchetti, and L. Radzihovsky, Phys. Rev. B **57**, 7705 (1998).
[8] A. E. Koshelev and V. M. Vinokur, Phys. Rev. Lett. **73**, 3580 (1994).
[9] K. Moon, R. T. Scalettar, and G. T. Zimanyi, Phys. Rev. Lett. **77**, 2778 (1996).
[10] C. J. Olson and C. Rechhardt, Phys. Rev. B **61**, R3811 (2000).
[11] H. Fangohr, S. J. Cox, and P. A. J. de Groot, Phys. Rev. B **64**, 064505 (2001).
[12] M. Chandran, R. T. Scalettar, and G. T. Zimanyi, Phys. Rev. B **67**, 052507 (2003).
[13] T. Giamarchi and P. Le Doussal, Phys. Rev. Lett. **76**, 3408 (1996); Phys. Rev. B **57**, 11356 (1998).
[14] E. H. Brandt, Rep. Prog. Phys. **58**, 1465 (1995).
[15] D. Li and B. Rosenstein, Phys. Rev. B **60**, 9704 (1999).
[16] C. Caroli and K. Maki, Phys. Rev. **164**, 591 (1967).
[17] R. S. Thompson and C.-R. Hu, Phys. Rev. Lett. **27**, 1352 (1971).
[18] R. J. Troy and A. T. Dorsey, Phys. Rev. B **47**, 2715 (1993).
[19] M. Tinkham, *Introduction to Superconductivity* (McGraw-Hill, New York, 1996).
[20] T. Blum and M. A. Moore, Phys. Rev. B **56**, 372 (1997).
[21] G. Lasher, Phys. Rev. **140**, A523 (1965).
[22] J. B. Ketterson and S. N. Song, *Superconductivity* (Cambridge University Press, Cambridge, 1999), Chap. 21.
[23] A. Ikeda, T. Ohmi, and T. Tsuneto, J. Phys. Soc. Jpn. **59**, 1740 (1990); **61**, 254 (1992); A. Ikeda, *ibid.* **64**, 1683 (1994); **64**, 3925 (1995).
[24] C. Villard, C. Peroz, and A. Sulpice, J. Low Temp. Phys. **131**, 516 (2003); C. Peroz *et al.*, Physica C **369**, 222 (2002).
[25] A. Tonomura, J. Low Temp. Phys. **131**, 941 (2003).